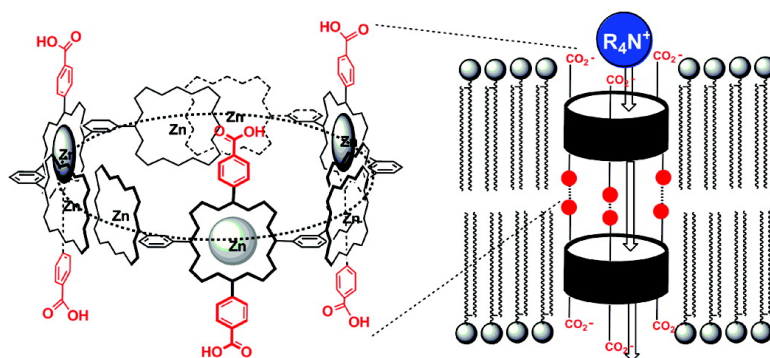


Transmembrane Nanopores from Porphyrin Supramolecules

Akiharu Satake, Mika Yamamura, Masafumi Oda, and Yoshiaki Kobuke

J. Am. Chem. Soc., **2008**, 130 (20), 6314-6315 • DOI: 10.1021/ja801129a • Publication Date (Web): 26 April 2008

Downloaded from <http://pubs.acs.org> on February 8, 2009



More About This Article

Additional resources and features associated with this article are available within the HTML version:

- Supporting Information
- Links to the 3 articles that cite this article, as of the time of this article download
- Access to high resolution figures
- Links to articles and content related to this article
- Copyright permission to reproduce figures and/or text from this article

[View the Full Text HTML](#)

Transmembrane Nanopores from Porphyrin Supramolecules

Akiharu Satake,* Mika Yamamura, Masafumi Oda, and Yoshiaki Kobuke*[‡]

Graduate School of Materials Science, Nara Institute of Science and Technology,
Takayama 8916-5, Ikoma, Nara 630-0192, Japan

Received February 14, 2008; E-mail: satake@ms.naist.jp; kobuke@iae.kyoto-u.ac.jp

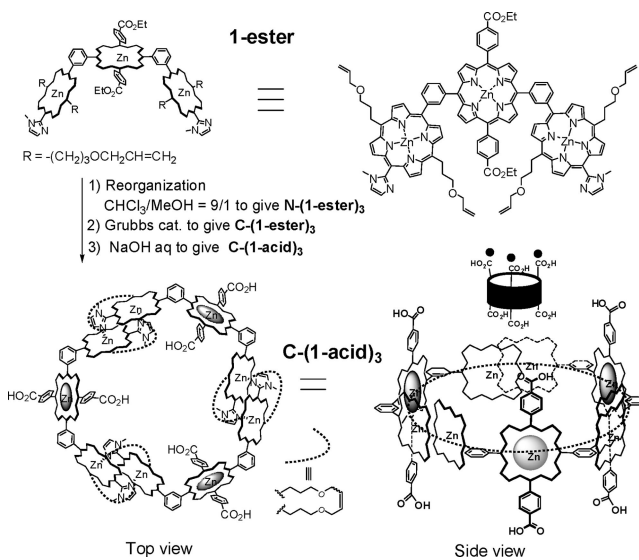
Molecular nanopores allowing passage through bilayer lipid membranes (BLM) have recently attracted much attention for applications in sensors, separation, reactors, and drug delivery systems.¹ Natural nanopores are generally defined as pores having diameters larger than 1 nm. They are significantly wider than conventional ion channels.² Although selective ion permeation is not expected through such a large pore, permeation of large molecules may open new possibilities. α -Hemolysin from natural sources provides a large pore (minimum diameter, D , 1.4 nm),³ and modification of inner pores⁴ allowed selective sensing of biologically important molecules, such as DNA⁵ and inositol 1,4,5-trisphosphate.⁶ Single-channel measurements are also powerful tools for detecting dynamic analyte transport behavior with single-molecule sensitivity.⁷ Creation of a pore large enough to exclude highly associative lipid components is generally difficult, and only smaller synthetic ion channels have been reported so far.^{8,9} As a limited example, Matile and his co-workers reported a barrel-stave nanopore ($D \sim 1.5$ nm) based on *p*-octiphenyl staves.^{10,11}

Recently, we reported porphyrin-based supramolecular macrocycles as mimics of photosynthetic light-harvesting antenna.^{12–14} The rigid skeletons of porphyrin, connected by orthogonal *m*-phenylene moieties, must be robust enough to keep their ring structure even in BLM. Herein, we designed a synthetic nanopore composed of **C-(1-acid)₃**, having six carboxylic acid groups directed up and down. The height of **(1-acid)₃** is estimated as 21 Å from the molecular model (Figure S1), corresponding to almost half the thickness of a BLM. Therefore, if two macrorings interact within a BLM by three cooperative hydrogen bonds, a transmembrane nanopore will be generated. Three carboxylic acids at the other ends will be appropriate as terminal ionic groups exposed to the aqueous layer.

Trisporphyrin ester **1-ester** was synthesized by palladium-catalyzed Suzuki–Miyaura coupling reaction of boronic ester appended imidazolylporphyrin **2** (2 equiv), *meso*-dibromoporphyrin **3** (1 equiv), and subsequent zinc ion insertion (Scheme S2). Trisporphyrin **1-ester** was organized into the cyclic trimer, **N-(1-ester)₃** according to an established method.^{13,14} The **N-(1-ester)₃** includes geometric isomers concerning the imidazole–zinc coordinations.^{13,14} The trimers were covalently linked by olefin metathesis using a first-generation Grubbs catalyst to give **C-(1-ester)₃**. Six ester groups in **C-(1-ester)₃** were hydrolyzed to yield **C-(1-acid)₃** (Schemes 1 and S3). The MALDI-TOF mass spectrum of **C-(1-acid)₃** showed the corresponding hexacarboxylic acid derivative peak, and the UV–vis spectrum of **C-(1-acid)₃** was almost identical to those of **N-(1-ester)₃** and **C-(1-ester)₃**, indicating that the ring structure was maintained through the reaction sequence.

Soybean lecithin based BLM containing **C-(1-acid)₃** was prepared at a pinhole on a plastic cell (Figure 1, left). Since **C-(1-acid)₃** was premixed in soybean lecithin, hydrogen bonds might be formed before its introduction into the cell. Then, only carboxylic acid groups exposed

Scheme 1. Synthesis of **C-(1-acid)₃**



to the aqueous layer were deprotonated during preparation of BLM. The ion channel current was recorded under symmetric salt conditions (*trans/cis* 500 mM KCl, pH 7.2) by applying various voltages. A typical ion current profile and I – V plot are shown in Figure S2 and Figure 1 (right), respectively. Very stable ion current was observed, and no open–close transition was detected. Conductivities, determined from slopes of I – V plots, varied from several tens of picosiemens to a few nano Siemens for different experimental runs. The fluctuation probably reflects differences in the number and/or the states of open pore(s) in each experimental run. These phenomena are generally observed in synthetic ion channels.^{15–17} No ion channel current was observed when **C-(1-ester)₃** was used instead of **C-(1-acid)₃**. Thus, the carboxylic acid groups are essential for forming the transmembrane nanopore. Ion currents were observed also for solutions of symmetric 500 mM LiCl and CaCl₂ as well as KCl. The large hydration energy

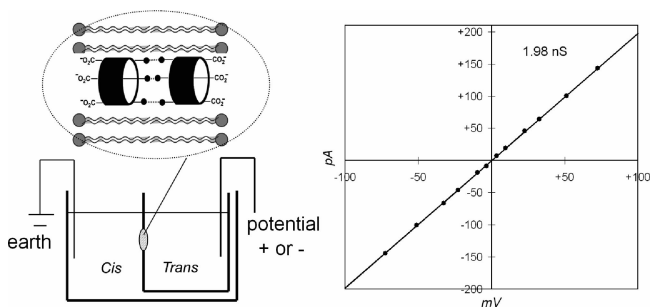


Figure 1. (Left) Schematic image of sample chambers separated by bilayer lipid membrane (BLM) including **C-(1-acid)₃** as an ion channel. (Right) A typical I – V plot of ion channel current of **C-(1-acid)₃** under 500 mM KCl symmetric conditions at pH 7.2. The slope indicates the conductivity of 1.98 nS.

[‡] Present address: Institute of Advanced Energy, Kyoto University, Gokasho, Uji 611-0011, Japan.

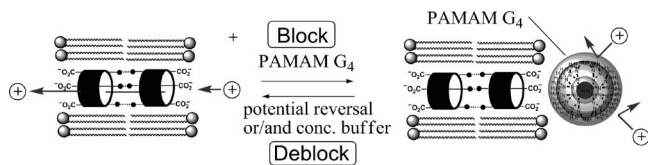


Figure 2. Schematic image of blocking by PAMAM dendrimer G_4 (G_4).

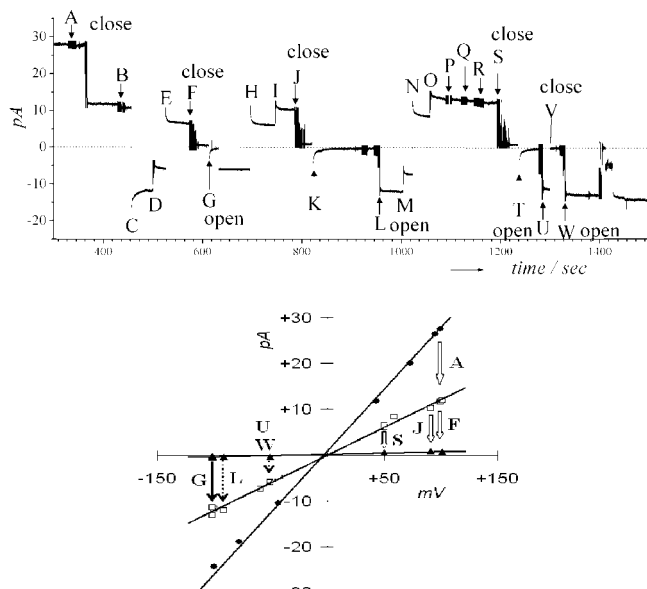


Figure 3. (Top) Time profile of blocking and deblocking of ion channel current. Conditions: 500 mM Me₄NCl, pH 7.2. (Bottom) I - V plots of the profile: (A) addition of G_4 (56 nM) at +100 mV, decrease of conductivity; (B) addition of G_4 (56 nM), no response; (C) -100 mV; (D) -50 mV; (E) +50 mV; (F, J) addition of G_4 (56 nM), closing channel; (G) -50 mV, then opening channel; (H) +50 mV; (I) +91 mV; (K) -91 mV, no response; (L, U, W) addition of HEPES-Tris buffer (5 mM), opening channel; (M) -59 mV; (N) +59 mV; (O) +100 mV; (P, Q, R, S) addition of G_4 (56 nM), closing channel at S; (T) -100 mV, no response; (V) spontaneous closing of the channel.

of lithium and calcium ions (-131 and -397 kcal/mol), respectively,² normally prohibits these ions from passing through ion channels. Observation of large ionic current for these ions is strong evidence for the formation of a large pore in BLM. In addition, hydrophobic and bulky quaternary ammonium ions, tetramethylammonium and tetrabutylammonium chlorides (500 mM), also passed through the pore. Cation/anion selectivity was examined by using asymmetric salt conditions of *cis* 10 mM and *trans* 100 mM tetramethylammonium chloride. The reversal potential was negative (-28 mV), indicating a moderate cation selectivity (Figure S3).

To gain further insights into the nanopore, blocking and deblocking of the ion channel current were examined using a PAMAM dendrimer.¹⁸ A schematic image of the experiment is shown in Figure 2. During ion current observation with positive voltages applied, fourth-generation PAMAM dendrimer (G_4 , 26.7 Å radius)¹⁹ was added to the *trans* side. After the ion current was blocked, the applied potential was reversed and concentrated buffer solution was added to recover the ion current. The time profile and I - V plots of ion channel current are depicted in Figure 3. After confirming the ohmic I - V response (filled circles, 270 ps), 56 nM of G_4 was added at point A. Ion current decreased to less than half the original value. Ohmic response was observed between points B and F (120 ps). The current drifts observed at C, E, and others on investigating the bias potentials are due to charging current during formation of an electric double layer. Further addition of

dendrimer at F blocked the ion current almost completely. At G, the applied potential was inverted to make the *trans* side negative. The former conductivity was regenerated. The open state continued even if the applied potential was inverted to positive again (H and I). Blocking occurred again upon addition of G_4 at J, but reversal of potential application did not recover the open state (K). One drop of concentrated HEPES-Tris buffer was added to both *cis* and *trans* compartments to adjust the concentration to 10 mM at point L. Ion current was recovered again. Similar close and open transitions were repeated again at S and U.

The above experiment clearly shows that G_4 acted as a channel blocker. Blocking and deblocking mechanisms are explained as follows. Below pH 7.2, amino groups in the dendrimer are protonated and, thus, the dendrimers become polycationic. On the contrary, carboxylic acid groups in C-(1-acid)₃ are deprotonated at pH 7.2 and exposed to the aqueous phase. At positive applied voltages, polycationic dendrimers move toward the opposite electrode. They interact electrostatically with carboxylates at the pore entrance to block or perturb the ion flux. Application of reverse voltage or increased buffer concentration weakens the electrostatic interaction. Transitions between open and blocked states are clearly demonstrated by observing transmembrane ion current.

The present study clearly demonstrates stable nanopore formation from rigid porphyrin-based macrorings, through which large molecules are transferred across BLM.

Acknowledgment. This work was supported by Young Scientists (B) (A.S.) and Grants-in-Aid for Scientific Research (A) (Y.K.) from JSPS (Japan Society for the Promotion of Science).

Supporting Information Available: Experimental details of synthesis and ion channel measurement, molecular modeling, NMR and UV-vis spectra, and other data. This material is available free of charge via the Internet at <http://pubs.acs.org>.

References

- Bayley, H.; Braha, O.; Cheley, S.; Gu, L.-Q. In *Nanobiotechnology*; Niemeyer, C., Mirkin, C., Eds.; Wiley-VCH: Weinheim, Germany, 2004; Chapter 7, pp 93-112.
- Hille, B. *Ion Channels of Excitable Membranes*, 3rd ed.; Sinauer Associates: Sunderland, MA, 2001.
- Song, L. Z.; Hobaugh, M. R.; Shustak, C.; Cheley, S.; Bayley, H.; Gouaux, J. E. *Science* **1996**, *274*, 1859-1866.
- Martin, H.; Kinns, H.; Mitchell, N.; Astier, Y.; Madathil, R.; Howorka, S. *J. Am. Chem. Soc.* **2007**, *129*, 9640-9649.
- Cheley, S.; Gu, L. Q.; Bayley, H. *Chem. Biol.* **2002**, *9*, 829-838.
- Howorka, S.; Cheley, S.; Bayley, H. *Nat. Biotechnol.* **2001**, *19*, 636-639.
- Bayley, H.; Martin, C. R. *Chem. Rev.* **2000**, *100*, 2575-2594.
- Sisson, A. L.; Shah, M. R.; Bhosale, S.; Matile, S. *Chem. Soc. Rev.* **2006**, *35*, 1269-1286.
- Matile, S.; Som, A.; Sorde, N. *Tetrahedron* **2004**, *60*, 6405-6435.
- Bhosale, R.; Bhosale, S.; Bollot, G.; Gortea, V.; Julliard, M. D.; Litvinchuk, S.; Mareda, J.; Matile, S.; Miyatake, T.; Mora, F.; Perez-Velasco, A.; Sakai, N.; Sisson, A. L.; Tanaka, H.; Tran, D.-H. *Bull. Chem. Soc. Jpn.* **2007**, *80*, 1044-1057.
- Sakai, N.; Mareda, J.; Matile, S. *Acc. Chem. Res.* **2005**, *38*, 79-87.
- Takahashi, R.; Kobuke, Y. *J. Am. Chem. Soc.* **2003**, *125*, 2372-2373.
- Kuramochi, Y.; Satake, A.; Kobuke, Y. *J. Am. Chem. Soc.* **2004**, *126*, 8668-8669.
- Kuramochi, Y.; Satake, A.; Itou, M.; Ogawa, K.; Araki, Y.; Ito, O.; Kobuke, Y. *Chem.-Eur. J.* **2008**, *14*, 2827-2841.
- Goto, C.; Yamamura, M.; Satake, A.; Kobuke, Y. *J. Am. Chem. Soc.* **2001**, *123*, 12152-12159.
- Fyles, T. M.; Loock, D.; van Straaten-Nijenhuis, W. F.; Zhou, X. *J. Org. Chem.* **1996**, *61*, 8866-8874.
- Ishida, H.; Qi, Z.; Sokabe, M.; Donowaki, K.; Inoue, Y. *J. Org. Chem.* **2001**, *66*, 2978-2989.
- Tomalia, D. A. *Prog. Polym. Sci.* **2005**, *30*, 294-324.
- Lee, I.; Athey, B. D.; Wetzel, A. W.; Meixner, W.; Baker, J. R. *Macromolecules* **2002**, *35*, 4510-4520.

JA801129A